Predictions of Soot in Laminar Diffusion Flames

Ian M. Kennedy* and Wolfgang Kollmann†
University of California at Davis, Davis, California 95616
and
J.-Y. Chen‡
Sandia National Laboratories, Livermore, California 94551

A model for soot formation in diffusion flames is proposed in which a correlation between mixture fraction and soot surface growth rate is used. The correlation is derived from measurements in a stagnation point diffusion flame. The calculation solves the boundary-layer form of the flow equations, which include the continuity equation, momentum, mixture fraction, and the enthalpy equations. The latter equation is included to account for radiation, which earlier studies found to be important in determining the flame temperatures in sooty flames and the rates of soot reactions. Results are presented for two laminar flows. The first is an axisymmetric laminar jet diffusion flame and the second is a Wolfhard-Parker two-dimensional flame. Good agreement has been obtained for both flows without adjustment of the model parameters.

Nomenclature

a_p = Planck mean absorption coefficient
C_P = specific heat at constant pressure
D = diffusivity
E = activation energy
e_b = Planck's spectral distribution function
f = mixture fraction
g = gravitational acceleration
h = enthalpy
h_f° = heat of formation at standard state
k = absorption coefficient
N = particle number density
p = pressure
q = heat flux
R = gas constant
r = radial coordinate
S = specific surface growth rate
T = temperature
u = axial velocity
v = radial velocity
w_g = soot surface growth rate
w_n = soot inception rate
w_o = soot oxidation rate
Y = species mass fraction
λ = thermal conductivity
λ = wavelength in Eqs. (8) and (9)
ν = kinematic viscosity
ρ = gas density
ϕ = soot volume fraction

Subscripts

ad = adiabatic
i = species i
r = radiation
s = soot
t = thermophoretic
∞ = surroundings

Introduction

MOST combustion systems operate in a nonpremixed or diffusion flame mode. The most common fuels are the heavier hydrocarbons. This combination of conditions is conducive to the formation of soot. In many, but not all, combustion systems, the formation or emission of soot is undesirable for environmental and operational reasons. A great deal of research effort has been directed toward this problem, and in recent years, a better understanding of the underlying physical and chemical mechanisms has been obtained.[1,2] However, there have been few attempts to make use of this information in a predictive model of soot formation.

An early model was formulated by Jensen[3] in which he proposed a simple kinetic scheme for the formation of a C_2 nucleus that underwent subsequent growth and coagulation. His scheme suffered from the difficulty in trying to handle the chemistry of soot formation from first principles; considerable uncertainty still surrounds this topic and, furthermore, it leads to a numerical scheme that is too complicated to incorporate in a useful code for diffusion flame predictions.

Magnussen and Hjertager[4] used a simpler approach to predict soot concentrations in a turbulent acetylene diffusion flame. They made use of the kinetic scheme of Tesner et al.[5] for nuclei formation rates and surface growth rates. Gore and Faeth[6] attempted to develop a universal relationship between soot volume fraction and mixture fraction. They found that this approach was not viable in a laminar flame due to the complex history of soot particles in the flowfield. More recently, Moss et al.[7] modeled soot formation by solving for the rates of particle nucleation, soot surface growth rate, coagulation rate, and burnout rate; they accounted for the transport of soot particles by the flow.

Kennedy et al.[8] showed that reasonable predictions of soot loading in a laminar diffusion flame could be obtained by solving for the particle number density. They used an empirical correlation of soot growth rates with mixture fraction in the calculation so that detailed chemistry did not enter into the problem. The relationships between mixture fraction and the flow properties such as the density and the temperature were obtained from a detailed calculation of the stagnation point diffusion flame.[9] Two cases were investigated, viz., with a radiation heat loss and the adiabatic case. The radiation was introduced in an entirely ad hoc manner; the energy equation was not solved. It was found that the decrease in temperature that occurs with radiative energy loss has a significant impact on the soot loadings in these flames. Therefore, a more thorough approach to the problem of accounting for radiation in a diffusion flame was deemed necessary.

Presented as Paper 90-0459 at the AIAA 28th Aerospace Sciences Meeting, Reno, NV, Jan. 8-11, 1990; received Feb. 23, 1990; revision received Nov. 16, 1990; accepted for publication Nov. 19, 1990.

*Associate Professor, Department of Mechanical Engineering. Member AIAA.

†Professor, Department of Mechanical Engineering.

‡Research Scientist, Combustion Research Facility.

The present paper reports on the refinement of the earlier modeling approach by the addition of an energy equation with a radiative loss term. The thermochemistry, i.e., the correlation between the flow properties such as density, temperature, and viscosity, and the calculated variables (mixture fraction and enthalpy), has been determined through a constrained equilibrium approach. In order to give a thorough test of the model, it has been applied to two different laminar diffusion flame configurations. The first experiment that has been modeled is the axisymmetric ethylene diffusion flame of Santoro et al.[10] The other experiment is that of Kent and Wagner[11] who studied a laminar ethylene diffusion flame that was stabilized on a Wolfhard-Parker burner.

Flowfield Equations

The equations for the flow field include the continuity equation

$$\frac{\partial}{\partial x}(\rho u) + \frac{1}{r}\frac{\partial}{\partial r}(\rho r v) = 0 \tag{1}$$

and the boundary-layer form of the axial component of momentum

$$\rho u\frac{\partial u}{\partial x} + \rho v\frac{\partial u}{\partial r} = -\frac{\partial p}{\partial x} + \frac{1}{r}\frac{\partial}{\partial r}\left[\mu r\frac{\partial u}{\partial r}\right] + \rho g \tag{2}$$

Equation (2) may not be appropriate under all circumstances; for example, an axisymmetric flame that is only 1 or 2 diameters long will not satisfy the criteria for a boundary-layer type of flow due to significant diffusion in the axial direction. The flames that are investigated in this study approximate boundary-layer flows.

In order to keep the problem tractable, we do not solve for all species with detailed chemical kinetics and elementary reactions in the manner of Miller et al.[9] for stagnation point diffusion flames. Instead, we adopt the assumption that all species have the same diffusivities and their concentrations can be correlated with a mixture fraction.[12] The mixture fraction is a Shvab-Zeldovich variable[13] without a source or sink term. Its equation is as follows

$$\rho u\frac{\partial f}{\partial x} + \rho v\frac{\partial f}{\partial r} = \frac{1}{r}\frac{\partial}{\partial r}\left[\rho D r\frac{\partial f}{\partial r}\right] \tag{3}$$

Earlier work in this vein omitted the energy equation and introduced radiation effects in an ad hoc manner by calculating the mixture fraction-temperature correlation from the code[9] for a stagnation point diffusion flame with a sink term in the energy equation. The present work represents a significant improvement over that approach by including the energy equation directly with a radiation term. The energy equation is solved in terms of the total enthalpy, i.e., the sum of the chemical and sensible enthalpies

$$h = \sum_{i=1}^{N} h^{\circ}_{f,i} + \int_{T_o}^{T} C_{p_i}\,\mathrm{d}T \tag{4}$$

In terms of h, the steady, low Mach number form of the energy equation is

$$\rho u\frac{\partial h}{\partial x} + \rho v\frac{\partial h}{\partial r} = \frac{1}{r}\frac{\partial}{\partial r}\left[\frac{\lambda r}{C_P}\frac{\partial h}{\partial r} + r\left(\rho D - \frac{\lambda}{C_P}\right)\sum_{i=1}^{N} h_i\frac{\partial Y_i}{\partial r}\right] - \frac{\partial q}{\partial r} - \nabla\cdot q_r \tag{5}$$

Body forces and viscous dissipation have been ignored in Eq. (5). In Eq. (5), q is the radial component of the heat flux vector[12] without radiation. The radiative heat flux vector is q_r.

If it is assumed that all species have the same diffusivity and that the Lewis number is 1, then Eq. (5) reduces to

$$\rho u\frac{\partial h}{\partial x} + \rho v\frac{\partial h}{\partial r} = \frac{1}{r}\frac{\partial}{\partial r}\left[\frac{\lambda}{C_P} r\frac{\partial h}{\partial r}\right] - \nabla\cdot q_r \tag{6}$$

In most cases, the calculation of radiative heat fluxes is far from a trivial matter, particularly when the radiation is dominated by molecular emissions and absorption.[14] However, if the flame is sooty then the major part of its radiation is a continuum radiation that is simpler to model than the radiation due to water and carbon dioxide. For soot volume fractions $> \sim 10^{-7}$, soot radiation should be dominant judging by the calculations of Grosshandler and Modak.[15] For the small flames and moderate soot loadings with which we are dealing, the optically thin limit is appropriate. In this limit, the divergence of the radiative heat flux may be written as[16]

$$\nabla\cdot q_r = 4a_p\sigma(T^4 - T_\infty^4) \tag{7}$$

The Planck mean absorption coefficient may be calculated if the variation in soot absorption with wavelength is known. For this calculation, we have adopted the formula of Hottel and Sarofim[17] so that the absorption coefficient k is given by

$$k = \frac{7\phi}{\lambda} \tag{8}$$

where the wavelength is λ.

The Planck mean absorption coefficient may then be calculated for a given temperature and soot volume fraction ϕ as

$$a_p \equiv \frac{\int_0^\infty k(\lambda,\phi)\, e_b(\lambda)\,\mathrm{d}\lambda}{\int_0^\infty e_b(\lambda)\,\mathrm{d}\lambda} \tag{9}$$

Soot Model

In addition to the preceding equations, a further equation for the volume fraction of soot is required, viz.,

$$\rho u\frac{\partial \phi}{\partial x} + \rho(v + v_t)\frac{\partial \phi}{\partial r} = \frac{1}{r}\frac{\partial}{\partial r}\left(r\rho D_s\frac{\partial \phi}{\partial r}\right) + \rho w_n + \rho w_g - \rho w_o \tag{10}$$

In this equation, D_s is the diffusivity of soot particles, which is very small in reality but, in these calculations, it was found that without a small amount of diffusion some numerical oscillations were produced in the soot volume fraction results. D_s was taken to be 1% of the molecular diffusivity; variations around this value did not have an appreciable effect on the results other than to give smoother contours of volume fraction. The thermophoretic velocity v_T is calculated as[18]

$$v_T = -0.55\,\frac{\nu}{T}\frac{\partial T}{\partial r} \tag{11}$$

In keeping with the boundary-layer assumption, only the radial component of the thermophoretic velocity is considered; it is simply added to the convective velocity.

Soot surface growth rates w_g are determined by an empirical correlation between mixture fraction and the specific surface growth rate, i.e., the rate of growth per unit surface area of soot aerosol. The assumption is that surface growth rates are proportional to an aerosol surface area; reality may be somewhat more complicated in that growth may depend on the number of active sites that is not directly determined by surface area. However, for a given flame, it seems that the surface area hypothesis may afford the only possible modeling approach at present; previous experience[8,19] indicates that, at least in diffusion flames, this approach yields satisfactory results. The measurements of Axelbaum et al.[20] in a laminar stagnation point diffusion flame of ethylene were used to derive empirical values for the specific surface growth rate S as a function of the mixture fraction. More details may be found in Ref. 8. In order to account for the drop in temperature due to radiation, we have assumed that Arrhenius kinetics pertain to soot surface growth. An activation energy E of 20 Kcal/mole is used, and the local gas temperature is compared to the adiabatic equilibrium temperature to give the local specific surface growth rate $S(f,T)$; i.e., the empirical value of S is multiplied by a factor of exp $[-E/R(1/T - 1/T_{ad})]$, where T_{ad} is the adiabatic temperature at that point. Given the soot volume fraction ϕ and the number density of particles, the rate of growth is then

$$w_g = \pi^{1/3} 6^{2/3} N^{1/3} \phi^{2/3} \cdot S \tag{12}$$

It has been found by Kennedy et al.[8] that it is unnecessary to compute the particle number density from its own governing equation. Satisfactory results are obtained by assuming an average number density in Eq. (12) of 10^{16} m^{-3}, which corresponds to the typical number density that Axelbaum et al.[20] measured in their flame.

The rate of particle formation w_n in Eq. (10) is modeled on an ad hoc basis as a Gaussian distribution in mixture fraction space centered at a mixture fraction of $f = 0.1$. This value of f locates the particle production zone close to the reaction zone where particle inception is observed experimentally. The initial particle diameter was taken to be 1 nm, and the peak formation rate was 10^{18} m^{-3} s^{-1}. The details of this term were not found to be particularly important in determining the overall loading of soot in the flame. Particle oxidation has been included through the action of both OH radicals and O_2 although oxidation by OH was found to dominate in the present simulation of a diffusion flame. The rate of OH attack was evaluated from the free molecular collision rate between particle and molecule with a reaction probability of 5%; this value is about one half of the probability deduced by Neoh et al.[21] in their experiments. An ad hoc value of 5% produced improved results in the current simulation. The rate of O_2 attack was determined from the Nagle and Strickland-Constable formula.[22] Soot formation in the flames was calculated by integrating the set of coupled equations [Eqs. (1-3), (6), (10)] in a marching fashion[23] through the flowfield.

Constrained Equilibrium

For an adiabatic flame there are two choices for the thermochemistry that can be used in the calculations. One possibility is to use equilibrium values for the temperature, density, and viscosity. Another possibility is to use the correlation between these variables and the mixture fraction which can be evaluated from the detailed calculations of the laminar, stagnation point diffusion flame. The latter approach may be expected to give somewhat more realistic values for temperature, density, and composition than the equilibrium predictions.

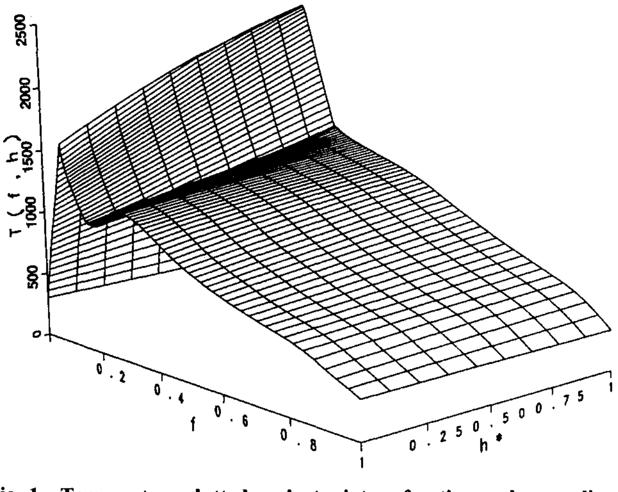

Fig. 1 Temperature plotted against mixture fraction and normalized enthalpy.

With strong energy losses due to radiation in the sooting diffusion flames, neither of these approaches is satisfactory. The temperature and other flow variables are functions of both mixture fraction and enthalpy in this case. Our solution has been to use a so-called constrained equilibrium approach to the problem. This consists of taking an equilibrium calculation and imposing a value of enthalpy on the problem; in essence, this can be thought of as cooling the system by some prescribed amount. A two-dimensional table of flow properties as functions of mixture fraction and enthalpy have been produced with this method. Figure 1 illustrates, for example, the relationship between temperature, mixture fraction, and a normalized enthalpy. In this figure, a normalized enthalpy of unity corresponds to the adiabatic enthalpy for a given mixture fraction and zero corresponds to a minimum likely enthalpy, which is chosen to be a few hundred degrees Kelvin above ambient. During the computation of a flame, these tables are interpolated to give the flow properties at a specified combination of the enthalpy and the mixture fraction.

Results

Two flows were modeled. The first was the flame of Santoro et al.[10] They burned ethylene on a cylindrical burner at a flow rate of 3.85 cc s^{-1}. Laser light scattering and extinction measurements were made of the soot volume fractions throughout the flame; a tomographic inversion technique was employed to convert the line-of-sight results into point measurements. The second configuration that we have investigated is the two-dimensional flame of Kent and Wagner.[11] In this case, an ethylene diffusion flame was stabilized on a Wolfhard-Parker burner. Again, laser light scattering and extinction methods were used to obtain values for the soot volume fractions and particle size. The results for this flame are somewhat less complete than for the flame of Santoro et al.[10]; therefore, attention will be directed primarily to the latter experiment.

The amount of soot that forms in a diffusion flame depends critically on the residence time or velocity field and the temperature field. The first criterion for a satisfactory model of these laminar flames is that it should predict these features of the flowfield satisfactorily. Of course, it must be borne in mind that the velocities are affected by the soot loading indirectly because these are buoyant flames. The amount of soot affects the temperatures in the flame and, consequently, the buoyancy driven flow is coupled to the soot calculation.

Figure 2 shows the radial profile of the axial component of velocity low in the flame of Santoro et al.[10] at 20 mm from the nozzle exit (the flame length is about 70 mm). The experimental results are also shown in this figure. A similar set of results are presented in Fig. 3 for a location at the end of the flame at 70 mm from the nozzle. This location was chosen so that the accuracy of the flowfield calculation could be demonstrated over the length of the flame. In particular, the effect of buoyancy on the velocity field is clearly demonstrated by comparison of Figs. 2 and 3.

Temperature profiles are shown for the same two locations in Figs. 4 and 5 along with the temperature measurements made by Santoro et al.[10] Measurements of temperature in a sooty flame are prone to some uncertainty and they may underestimate the true temperature. Predictions of the temperature field depend greatly on the coupled soot field as well as the assumptions about the thermochemistry.

Detailed data which were gathered in the experiment have been made available to us by Santoro.[24] The experimental results for soot volume fraction at 20 and 40 mm from the nozzle exit are plotted in Figs. 6 and 7, respectively. Also shown in these figures are our predictions of the soot volume fractions for this flame. The soot volume fractions at 70 mm

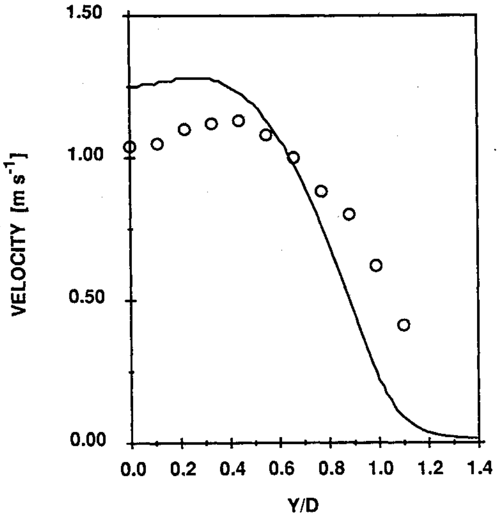

Fig. 2 Radial profile of axial velocity component at 20 mm in flame[10]: o measurements; —— predictions.

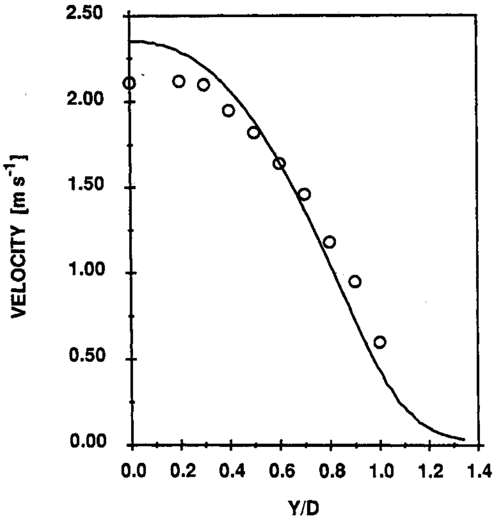

Fig. 3 Radial profile of axial velocity component at 70 mm in flame[10]: o measurements; —— predictions.

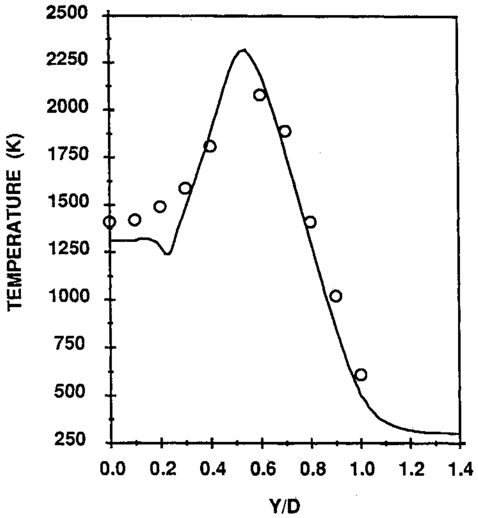

Fig. 4 Radial profile of temperature at 20 mm in flame[10]: o measurements; —— predictions.

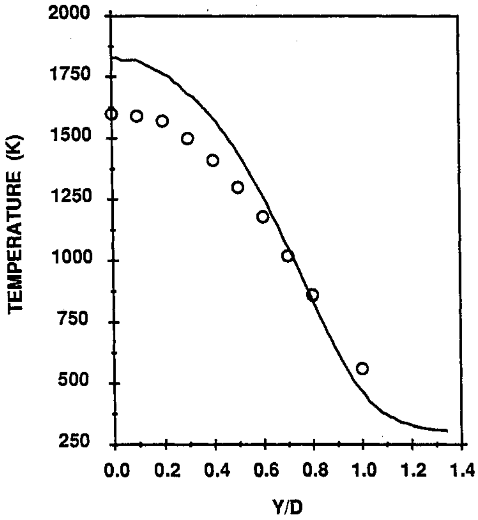

Fig. 5 Radial profile of temperature at 70 mm in flame[10]: o measurements; —— predictions.

(the flame tip) are not shown because the code predicts no soot to be emitted from the flame. On the other hand, the measurements revealed the presence of soot beyond the tip of the flame. This indicates that our soot oxidation rate is too great; the most likely cause is uncertainty in the prediction of OH concentrations.

With sufficient adjustable parameters in a code, it is usually possible to do a reasonably good job of predicting at least one set of data. A more stringent test of a model is whether it can perform as well in a completely different situation without any further adjustment of the parameters. To this end, we have applied exactly the same model to the experiment of Kent and Wagner[11] for their Wolfhard-Parker configuration. Comparisons are drawn in Figs. 8 and 9 between the predictions of soot volume fraction and the light extinction measurements at locations of 50 and 110 mm from the burner lip, respectively.

Discussion

From the presentation of the velocity results, it may be seen that the present model does a good job of predicting the velocity field in these strongly buoyant flows. This is a necessary condition in order to achieve the correct residence times for particle growth. A further necessary condition is the prediction of the correct temperature. The results from the computer code are consistently higher than the measured values. It is likely that the measured values of the temperature are somewhat lower than the true temperature as a result of uncertainties in radiation loss corrections to thermocouple data. Temperature measurements in a sooty flame are also afflicted by the difficulty that results from the coating of beads by soot deposits. These deposits have the tendency to lower the thermocouple output as they increase in thickness. In addition, the use of the constrained equilibrium approach to obtain the flow properties in the calculation may yield an overestimate of the true temperature because, in practice, temperatures in a diffusion flame are usually a little less than the adiabatic equilibrium flame temperature. Despite the slight discrepancies in the measured and predicted velocity and temperature fields, it is reasonable to claim that the simple model that we have used performs well in reproducing the major features of the flame.

The agreement between the soot predictions and the measurements in Fig. 6 at 20 mm from the burner nozzle are quite good. The model predicts the correct soot loading and its distribution. However, at 40 mm from the nozzle, the predictions on the centerline are not as satisfactory. The measurements indicate substantial amounts of soot on the centerline at this position, whereas the numerical predictions indicated very little soot. The thermophoretic velocity was doubled to see if this was a factor, but the predicted soot volume fraction on the centerline was still much less than the measurements indicate. At this time, the discrepancy in the centerline results is unresolved; it should be pointed out that the uncertainty in the tomographic scheme that was used to invert the line-of-sight data probably has its greatest errors at locations near the centerline. A further source of potential discrepancy lies in the correlation of growth rates with a Shvab-Zeldovich variable, viz., the mixture fraction. Saito et al.[25] found that soot precursors and growth species were poorly correlated with mixture fraction. The concentrations of these species increased with distance along the axis of a round, laminar methane flame. Residence times in the axisymmetric diffusion flame are much longer than in the counterflow flame that was used to develop the soot growth rate correlations. One may expect that regions of particle formation and growth broaden to larger values of the mixture fraction as residence times increase.

A further discrepancy between the predictions and the measurements concerns the emission of soot from the flame. The ability to predict correctly the conditions under which a flame will emit soot is quite obviously very desirable. In order to do this, it is necessary to predict both soot formation rates and soot burnout rates accurately. It appears from our results that the kinetics that we have adopted overestimate the rate of soot oxidation. This may be due to a number of possible factors. The temperature may be overestimated; this would lead to excessive oxidation rates and could account for the rapid burnout that we predict.

The model, as it has been set up, has only been tested up until now on laminar flames. The ultimate goal is to develop a useful model for the prediction of turbulent sooting diffusion flames. The relative simplicity of the model should be beneficial in this undertaking. Conventional turbulence models may run into a problem, however, in prescribing the form of the joint probability distribution function for the mixture fraction and the enthalpy. The simplest approach would be to assume statistical independence of the mixture fraction and the enthalpy. There is, however, no justification, a priori, for this assumption and it may lead to quite erroneous results. One may deduce the allowable values for the fluid state in enthalpy-mixture fraction space from physical reasoning. For example, the adiabatic equilibrium value for the total enthalpy at a given mixture fraction is an upper limit to allowable values of this variable. From such reasoning, one may construct a plausible form for the joint pdf, but considerable uncertainty persists with regard to its detailed form. These uncertainties may have a significant effect on predictions of the mean soot volume fractions. It appears that a formulation of the model in a form that is suitable for a probability distribution function (pdf) transport calculation[26] may be desirable.

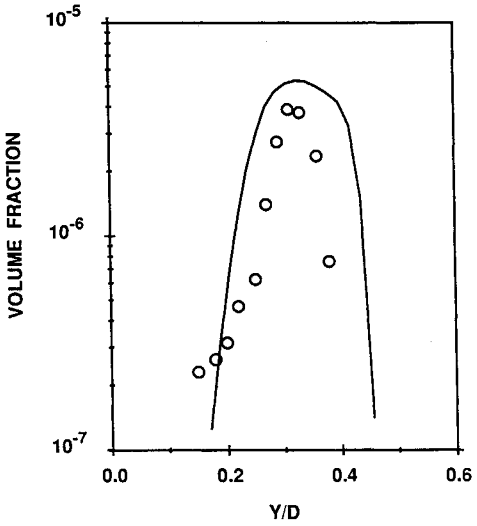

Fig. 6 Soot volume fraction profile at 20 mm in flame[10]: o measurements; —— predictions.

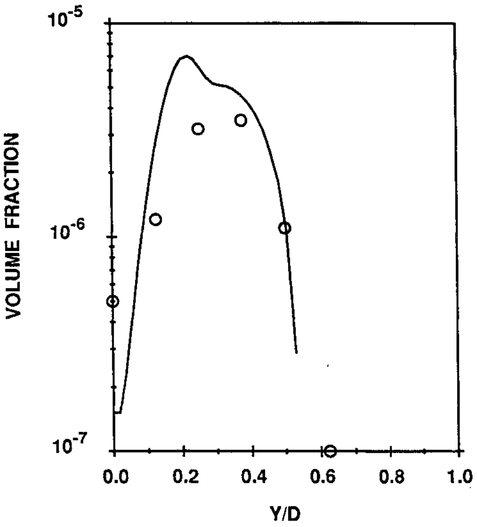

Fig. 8 Soot volume fraction profile at 50 mm in flame[10]: o measurements; —— predictions.

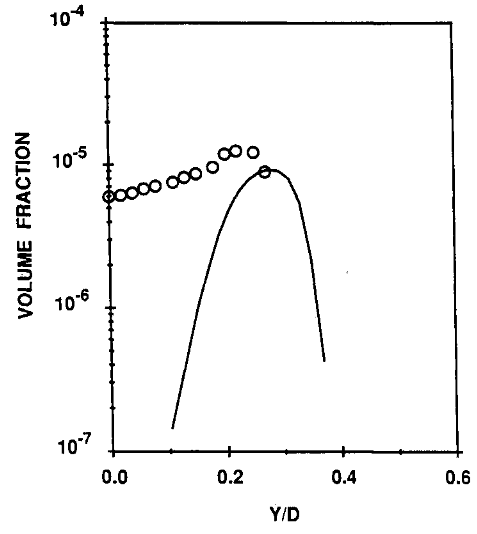

Fig. 7 Soot volume fraction profile at 40 mm in flame[10]: o measurements; —— predictions.

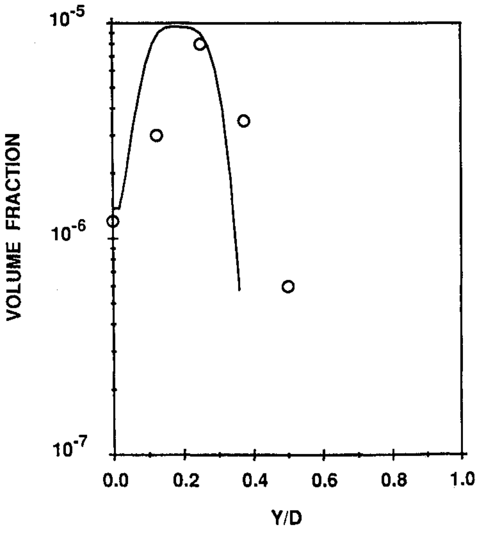

Fig. 9 Soot volume fraction profile at 110 mm in flame[10]: o measurements; —— predictions.

Conclusions

An earlier model for soot formation in a laminar diffusion flame has been improved by the addition of the energy equation that incorporates an optically thin model for soot radiation. The temperature, density, and viscosity have been determined as functions of the mixture fraction and the enthalpy by using a type of constrained equilibrium chemistry model. Although the concentrations are not predicted well with this chemistry model, the temperature, density, and viscosity are calculated sufficiently well to permit the flowfield to be predicted.

With the inclusion of radiation, there is a limiting process on the formation of soot. Because the surface growth reactions are presumed to have an activation energy, their rate decreases as the amount of soot increases and the temperature drops due to radiation. Accounting for this interaction has been found to be quite important.

The present model for soot formation is semiempirical and does not incorporate detailed chemistry. However, it is capable of doing a reasonable job of predicting soot loadings and the soot distribution in a diffusion flame. More important, it is apparently able to perform well in different flows without the adjustment of any parameters; this serves to give further confidence that it incorporates sufficient physics to describe the overall features of soot production in a laminar diffusion flame. The simplicity of the approach should permit its adaptation to a turbulent diffusion flame. The growth rate term in a conventional closure scheme may pose some difficulties because information would be needed on the joint pdf of mixture fraction and enthalpy. The model is formulated in a manner that is ideally suited for the application of a pdf transport scheme.

Acknowledgments

The first author wishes to acknowledge the support of a National Science Foundation Presidential Young Investigator Award CBT-8857477 and Aerojet TechSystems, Sacramento, California. At Sandia Laboratories, the work was supported by the U.S. Department of Energy, Office of Basic Energy Sciences. The cooperation of R. J. Santoro and NIST (formerly NBS) in supplying their detailed experimental results is appreciated.

References

[1] Haynes, B. S., and Wagner, H. Gg., "Soot Formation," *Progress in Energy and Combustion Science,* Vol 7, No. 4, 1981, pp. 229–273.

[2] Calcote, H. F., "Mechanisms of Soot Nucleation in Flames—A Critical Review," *Combustion and Flame,* Vol. 42, No. 3, 1981, pp. 215–242.

[3] Jensen, D. E., "Prediction of Soot Formation Rates: A New Approach," *Proceedings of the Royal Society of London, Series A.: Mathematical and Physical Sciences,* Vol. 338, No. 1612, London, 1974, pp. 375–396.

[4] Magnussen, B. F., "Modeling of Reaction Processes in Turbulent Flames with Special Emphasis on Soot Formation and Combustion," *Particulate Carbon,* edited by D. Siegla and G. Smith, Plenum, New York, 1981, pp. 321–334.

[5] Tesner, P. A., Snegiriova, T. D., and Knorre, V. G., "Kinetics of Dispersed Carbon Formation," *Combustion and Flame,* Vol. 17, Aug.-Dec. 1971, pp. 253–260.

[6] Gore, J. P., and Faeth, G. M., "Structure and Spectral Radiation Properties of Turbulent Ethylene/Air Diffusion Flames," *21st Symposium (International) on Combustion,* Combustion Institute, Pittsburgh, PA, 1986, pp. 1521–1531.

[7] Moss, J. B., Stewart, C. D., and Syed, K. J., "Flowfield Modeling of Soot Formation at Elevated Pressures," *22nd Symposium (International) on Combustion,* Combustion Institute, Pittsburgh, PA, 1988, pp. 413–423.

[8] Kennedy, I. M., Kollmann, W., and Chen, J.-Y., "A Model for Soot Formation in a Laminar Flame," *Combustion and Flame,* Vol. 81, No. 1, 1990, pp. 73–85.

[9] Miller, J. A., Kee, R. J., Smooke, M. D., and Grcar, J. F., "The Computation of the Structure and Extinction Limit of a Methane-Air Stagnation Point Diffusion Flame," Western States Section Meeting of the Combustion Institute, Paper WSS/CI 84-10, April 1984.

[10] Santoro, R. J., Yeh, T. T., Horvath, J. J., and Semerjian, H. G., "The Transport and Growth of Soot Particles in Laminar Diffusion Flames," *Combustion Science and Technology,* Vol. 53, No. 3, 1987, pp. 89–115.

[11] Kent, J. H., and Wagner, H. Gg., "Soot Formation in a Laminar Diffusion Flame," *18th Symposium (International) on Combustion,* Combustion Institute, Pittsburgh, PA, 1981, pp. 1117–1126.

[12] Bilger, R. W., "Turbulent Jet Diffusion Flames," *Progress in Energy and Combustion Science,* Vol. 1, No. 1, 1976, pp. 87–109.

[13] Williams, F. A., *Combustion Theory,* 2nd ed., Cummings, Menlo Park, CA, 1985.

[14] Viskanta, R., and Menguc, M. P., "Radiation Heat Transfer in Combustion Systems, " *Progress in Energy and Combustion Science,* Vol. 13, No. 2, 1987, pp. 97–160.

[15] Grosshandler, W. L., and Modak, A. T., "Radiation from Nonhomogeneous Combination Products," *18th Symposium (International) on Combustion,* Combustion Institute, Pittsburgh, PA, 1981, pp. 601–609.

[16] Siegel, R., and Howell, J. R., *Thermal Radiation Heat Transfer,* 2nd ed., Hemisphere, Washington, DC, 1981.

[17] Hottel, H. C., and Sarofim, A. F., *Radiative Transfer,* McGraw-Hill, New York, 1967.

[18] Talbot, L., Cheng, R. K., Schefer, R. W., and Willis, D. R., "Thermophoresis of Particles in a Heated Boundary Layer," *Journal of Fluid Mechanics,* Vol. 101, Pt. 4, 1980, pp. 737–758.

[19] Kennedy, I. M., "Soot Aerosol Dynamics in a Stagnation Point Diffusion Flame," *20th Symposium (International) on Combustion,* Combustion Institute, Pittsburgh, PA, 1984, pp. 1095–1104.

[20] Axelbaum, R. L., Flower, W. L., and Law, C. K., "Dilution and Temperature Effects of Inert Addition on Soot Formation in a Counterflow Diffusion Flame," *Combustion Science and Technology,* Vol. 61, No. 1, 1988, pp. 51–74.

[21] Neoh, K. G., Howard, J. B., and Sarofim, A. F., "Soot Oxidation in Flames," *Particulate Carbon Formation During Combustion,* edited by D. Siegla and G. Smith, Plenum, N.Y., 1981, p. 261–282.

[22] Nagle, J., and Strickland-Constable, R. F., "Oxidation of Carbon Between 1000–2000°C," *Proceedings of the 5th Conference on Carbon,* Pergamon, London, 1962, pp. 154–164.

[23] Chen, J.-Y., Kollmann, W., and Dibble, R. W., "Numerical Computations of Turbulent Free-Shear Flows using a Block-Tridiagonal Solver for a Staggered Grid System," *Proceedings of the 18th Annual Pittsburgh Conference on Modeling and Simulation,* Instrument Society of America, Pittsburgh, PA, 1987, pp. 1833–1837.

[24] Santoro, R. J., private communication, 1989.

[25] Saito, K., Williams, F. A., and Gordon, A. S., "Structure of Laminar Co-Flow Methane-Air Diffusion Flames," *Journal of Heat Transfer,* Vol. 108, No. 3, 1986, pp. 640–648.

[26] Pope, S. B., "PDF Methods for Turbulent Reactive Flows," *Progress in Energy and Combustion Science,* Vol. 11, No. 2, 1985, pp. 119–192.